

Mill Island warming

J. L. Roberts et al.

This discussion paper is/has been under review for the journal The Cryosphere (TC).  
Please refer to the corresponding final paper in TC if available.

# Borehole temperatures reveal a changed energy budget at Mill Island, East Antarctica over recent decades

J. L. Roberts<sup>1,2</sup>, A. D. Moy<sup>1,2</sup>, T. D. van Ommen<sup>1,2</sup>, M. A. J. Curran<sup>1,2</sup>,  
A. P. Worby<sup>3</sup>, I. D. Goodwin<sup>4</sup>, and M. Inoue<sup>2,5</sup>

<sup>1</sup>Department of Sustainability, Environment, Water, Population and Communities,  
Australian Antarctic Division, Hobart, Tasmania, Australia

<sup>2</sup>Antarctic Climate and Ecosystems Cooperative Research Centre, University of Tasmania,  
Private Bag 80, Hobart, Tasmania 7001, Australia

<sup>3</sup>CSIRO Marine and Atmospheric Research, Castray Esplanade, Hobart,  
Tasmania 7000, Australia

<sup>4</sup>Marine Climate Risk Group, Department of Environment and Geography, Macquarie  
University, Eastern Road, Macquarie University, New South Wales 2109, Australia

<sup>5</sup>Institute for Marine and Antarctic Studies, University of Tasmania, Private Bag 129, Hobart,  
Tasmania 7001, Australia

Received: 8 June 2012 – Accepted: 28 June 2012 – Published: 18 July 2012

Correspondence to: J. L. Roberts (jason.roberts@aad.gov.au)

Published by Copernicus Publications on behalf of the European Geosciences Union.

Title Page

Abstract

Introduction

Conclusions

References

Tables

Figures

◀

▶

◀

▶

Back

Close

Full Screen / Esc

Printer-friendly Version

Interactive Discussion



## Abstract

A borehole temperature record from the Mill Island (East Antarctic) icecap reveals a large surface warming signal manifested as a 0.75 K temperature difference over the approximate 100 m depth below the seasonally varying zone. The temperature profile shows a break in gradient between 49 and 69 m depth, which we model with inverse numerical simulations, indicating that surface warming started around the austral summer of 1980/1981 AD  $\pm$  5 yr. This warming of approximately 0.37 K per decade is large by Antarctic standards and is only exceeded in regions of the Antarctic Peninsula. While this warming may reflect regional scale air temperature increases, the lack of comparable trends for other East Antarctic sites suggests local influences are largely responsible for the observed trend. Alteration of the surface energy budget arising from changes in radiation balances due to local cloud, the amount of liquid deposition and local air temperatures associated with altered air/sea exchanges potentially play a key role at this location due to the proximity of the Shackleton Ice Shelf and sea-ice zone.

## 1 Introduction

Palaeoclimate records provide an essential context for present day climate, and help us to understand the drivers of climate change. Ice core records from Antarctica have provided insights into the cycle of glacial and interglacial periods as far back as 800 000 yr (Jouzel et al., 2007) and show how the ice sheets have responded to past changes in temperature. However a lack of high-resolution climate data, especially for the Southern Hemisphere (Mann and Jones, 2003; Neukom and Gergis, 2012), still limits our understanding of climate processes over the past several millennia. In particular, while recent Northern Hemisphere temperatures have, on average, been warmer than any-time in at least the last 1300 yr (Mann and Jones, 2003; Mann et al., 2008), the recent Southern Hemisphere warming is only of comparable size to the relatively large uncertainties (likely because of data sparsity) in palaeo-reconstructions for the Southern

TCD

6, 2575–2595, 2012

## Mill Island warming

J. L. Roberts et al.

Title Page

Abstract

Introduction

Conclusions

References

Tables

Figures

◀

▶

◀

▶

Back

Close

Full Screen / Esc

Printer-friendly Version

Interactive Discussion



Hemisphere (Mann and Jones, 2003; Mann et al., 2008). Records from sites such as Mill Island help address this data sparsity and provide insights into the rate of change over the past century.

While spatially isolated temperature reconstructions are useful for investigating local changes in climatic conditions, consistent features of regional scale climatic conditions can be reconstructed with a spatially distributed network of observations. In particular, the Mill Island record is situated partway between Law Dome and the Vestfold Hills where a relationship between Law Dome summer temperature and evaporation in Ace Lake in the Vestfold Hills has previously been reported (Roberts et al., 2001). There are very limited data records available for this broad region of East Antarctica before the 1957–1958 International Geophysical Year, so that palaeo-reconstructions are required to assess the long-term regional climate history. Furthermore, this is the most northerly region of Antarctica outside the tip of the Antarctic Peninsula, and therefore a Mill Island temperature reconstruction represents the most northerly temperature record for East Antarctica.

## 2 Temperature observations

Mill Island is located at 65°30' S, 100°40' E (see Fig. 1), just offshore from the Bunger Hills in East Antarctica and bordering the Shackleton Ice Shelf. In the summer of 2009/2010 the Australian Antarctic program drilled a 120 m deep ice core as part of an ongoing program to obtain palaeoclimate records from a network of East Antarctic sites for the purpose of reconstructing regional-scale climate, including temperature, precipitation and circulation indices. The high temporal resolution, due to the high snow fall rates of  $1312 \text{ kg m}^{-2} \text{ yr}^{-1}$  at this site, and other high accumulation coastal sites in East Antarctica, including Law Dome, makes these sites particularly valuable for obtaining detailed climate records.

In summer of 2010/2011 a field party returned to Mill Island to measure the temperatures in the dry borehole (65°33'25.84" S, 100°47'11.44" E and ice surface elevation of

### Mill Island warming

J. L. Roberts et al.

Title Page

Abstract

Introduction

Conclusions

References

Tables

Figures

◀

▶

◀

▶

Back

Close

Full Screen / Esc

Printer-friendly Version

Interactive Discussion



503 above mean sea-level), which was capped in the summer 2009/2010. The dry-hole temperature measurements were made using a Leeds and Northrup resistance bridge to measure the resistance of a four-wire platinum probe. Measured resistances were converted to temperature using the standard relation for industrial platinum temperature sensors. The platinum probe was coupled to a rope marked with 1–5 m graduations, and weighted to ensure the sensor tip was in contact with the ice wall of the borehole. Temperature readings are shown in Table 1. The borehole temperature measurements have an instrumental accuracy of approximately 0.02 °C. All measured depths are relative to the 2010/2011 surface and ages are calculated from this datum.

The observed temperature distribution in the borehole is shown in Table 1. Surface temperature variations are known to propagate into ice sheets, with the attenuation of this temperature signal with depth being strongly influenced by the frequency of the surface variations (Patterson, 1994). Seasonal scale variations have attenuated to 5 % of the surface amplitude at around 10 m below the surface and are “undetectable below a depth of 20 m” (Patterson, 1994). Therefore we discarded the upper three measurements when assessing the trend in Mill Island surface energy budget.

### 3 Numerical model

To reconstruct a surface temperature history that is consistent with the observed temperature profile down the borehole, a forward numerical model (see Sect. 3.1) was developed that simulates the down borehole temperature profile given a surface temperature history, taking into account advection, thermal diffusion and the heat associated with firn densification (contributing up to 0.06 K in these simulations). Two inverse models that optimises surface temperature histories to minimise (in a least squares sense) the mismatch between the simulated and observed down borehole temperature profiles are described. One of these inverse models, the Least Squares QR (LSQR) model (see Sect. 3.2.1), is computationally very efficient and produces a single optimal solution with minimal variance, while the second method, the Particle Swarm Optimisation

## Mill Island warming

J. L. Roberts et al.

Title Page

Abstract

Introduction

Conclusions

References

Tables

Figures



Back

Close

Full Screen / Esc

Printer-friendly Version

Interactive Discussion



(PSO) method (see Sect. 3.2.2), requires significantly more computational resources, but produces a distribution of likely temperature reconstructions.

### 3.1 Forward model

The equation for the evolution of temperature ( $T$ ) with time ( $t$ ) in the absence of horizontal advection is (see Sect. 6 for nomenclature)

$$\frac{\partial T}{\partial t} = \frac{\kappa}{\rho C} \frac{\partial^2 T}{\partial z^2} + \frac{1}{\rho C} \left( \frac{\partial \kappa}{\partial z} - \rho C w \right) \frac{\partial T}{\partial z} + \frac{f}{\rho C} \quad (1)$$

Where the last term is the energy associated with firn densification (Patterson, 1994, Chap. 10, Eq. 32). We use a linear relationship for the specific heat capacity, namely  $C = 152.5 + 7.122T$  (Patterson, 1994, Chap. 10, Eq. 1). The thermal conductivity in ice is taken as  $K = 9.828 \exp(-5.7 \times 10^{-3}T)$  and as per van Ommen et al. (1999), the thermal conductivity of the firn is the arithmetic average of the lower bound of Van Dusen (Patterson, 1994, Chap. 10, Eq. 3) and the upper bound of Schwerdtfeger (Patterson, 1994, Chap. 10, Eq. 4). The firn densification term in Eq. (1) is given by  $f = \frac{wg}{\rho} \frac{\partial \rho}{\partial z} \int_0^z \rho(\gamma) d\gamma$ . We applied Sorge's Law (time invariant firn density profile) to piecewise exponential plus linear or dual exponential (cross-over at 57 m) empirical fit to the measured density profile (see Fig. 2a), extrapolated beyond the depth of the Mill Island ice core using densities from the deep ice core at Law Dome Summit (van Ommen et al., 1999).

The thermal boundary conditions applied to the model were a time varying, prescribed surface temperature, and a zero heat flux boundary condition at depth. The optimal surface temperature history was found to be essentially independent of the location of this bottom boundary condition for depths in excess of 180 m below the surface (see below).

The vertical velocity distribution with depth is unknown, but the resulting reconstruction of surface temperature history is essentially independent of reasonable assumed velocity profiles. In particular, we assume that the surface vertical velocity is equal to the recent snow accumulation rate of  $2.93 \text{ m yr}^{-1}$  at a surface snow density of  $448 \text{ kg m}^{-3}$ .

## Mill Island warming

J. L. Roberts et al.

Title Page

Abstract

Introduction

Conclusions

References

Tables

Figures

◀

▶

◀

▶

Back

Close

Full Screen / Esc

Printer-friendly Version

Interactive Discussion



**Mill Island warming**

J. L. Roberts et al.

[Title Page](#)[Abstract](#)[Introduction](#)[Conclusions](#)[References](#)[Tables](#)[Figures](#)[◀](#)[▶](#)[◀](#)[▶](#)[Back](#)[Close](#)[Full Screen / Esc](#)[Printer-friendly Version](#)[Interactive Discussion](#)

We assume a Nye style velocity profile (constant vertical strain rate) and correct for firm density. Assuming that the base of the ice sheet is approximately at sea-level, gives a maximum depth of around 400 m, and allowing a typical 5/6 factor between the actual and effective depths, gives a maximum effective Nye depth for the velocity profile of 333 m. This was the default velocity profile used, a second profile with an effective Nye depth of 200 m was used to test the model sensitivity to this parameter (see Sect. 3.3), Fig. 2b shows these two velocity profiles.

A finite difference implementation of Eq. (1) was used to simulate the temperature profile with depth under the influence of a time varying surface temperature. The finite difference scheme was second order in space and first order in time with a forward time discretisation used to simulate 130 yr, with the initial 10 yr discarded to minimise in impact of transients associated with inconsistent initial conditions.

## 3.2 Inverse models

### 3.2.1 LSQR reconstruction

The LSQR method uses an iterative greedy algorithm which reduces the largest temperature residual in each iteration. The sensitivity matrix for the response of the temperature at the depth of the largest residual to the surface temperature history was calculated using the Complex-Step derivative approximation (Martins et al., 2003). The surface temperature history is incremented by the minimum variance solution of this residual equation using a least squares QR method (Paige and Saunders, 1982). The initial temperature history was a linear interpolation of the measured temperature profile with the depth mapped to time using the assumed vertical velocity profile.

### 3.2.2 PSO reconstruction

Particle Swarm Optimisation solves for a group of particles (15 in this case) that traverse the parameter space being drawn towards the best solution (lowest RMS error)

**Mill Island warming**

J. L. Roberts et al.

Title Page

Abstract

Introduction

Conclusions

References

Tables

Figures

I◀

▶I

◀

▶

Back

Close

Full Screen / Esc

Printer-friendly Version

Interactive Discussion



that any of the particles has visited (Pedersen and Chipperfield, 2010). In order to suppress unresolved high frequency variations, a piecewise linear surface temperature history was used, with 4 linear segments. Once any of the solutions has achieved an RMS error below a specified threshold, the best ground surface temperature history corresponding to the best RMS error is saved, and a new swarm generated with a new randomised initial state. Five hundred such swarms were simulated for varying specified RMS thresholds, with a RMS threshold of  $0.05^{\circ}\text{C}$  being an optimum (see Sect. 3.3), and the median and distributions of these swarms analysed.

### 3.3 Numerical convergence

Numerical convergence was tested using an inverse model to calculate the required surface temperature history corresponding to the observed temperature profile, specifically using the the LSQR solution method (see Sect. 3.2.1). In particular the three key assumptions of the numerical scheme (numerical spatial resolution, effective Nye depth and the depth of the bottom zero heat flux boundary condition) were tested for the influence on the reconstructed surface temperature history. For these tests we will exclude the more recent decade of the reconstruction, where we have little data to constrain the solution for this period (see Sect. 2).

Grid independence was tested using a 180 m computational domain with either 2 m or 5 m discretisation. The RMS difference between the reconstructed temperature histories was  $0.057^{\circ}\text{C}$ . Most of the variation was in the upper part of the profile, where the approximately 2 m spacing of the measurements meant, that for the 5 m discretisation case, a sensitivity matrix could not be generated for each of the observational depths independently.

The influence of the location of the bottom zero flux boundary condition was investigated using a 2 m spatial grid with domains of 180 m, 250 m and 350 m depth and the zero heat flux boundary condition applied at the bottom of the computational domain (see Fig. 3). The RMS temperature difference between the 180 m and 350 m domains is  $0.040^{\circ}\text{C}$ , while between the 250 m and 350 m domains this is reduced to  $0.015^{\circ}\text{C}$ .

So we conclude that there is a slight dependence on the location of the zero heat flux boundary condition for shallow computational domains, but for domains of at least 250 m extent, the reconstructed ground surface temperature becomes independent of the computational domain size.

5 The influence of the effective Nye depth was studied using a 2 m spatial grid with a computational domain of 180 m and varying the velocity profile to have an effective Nye depth of either 200 or 333 m. The shallow computational domain was used to avoid unrealistic vertical velocities at depth as a result of the 200 m the Nye depth. The respective surface temperature histories differ by 0.039 °C, with the deeper effective  
10 Nye depth being slightly cooler throughout most of the history.

The sensitivity of the PSO solution to the specified RMS threshold is shown in Table 2. As expected, the RMS error of the median solution decreases with a decreasing RMS threshold, but for low RMS thresholds the resulting distribution from the swarms is noticeably skewed and the maximum error in the median solution increases for these  
15 skewed distributions. Therefore the optimal value for the RMS threshold was chosen as 0.05 °C.

#### 4 Surface temperature reconstruction

Estimations of the ground surface temperature history were obtained by minimising the root mean square (RMS) error in the temperature profile with depth obtained using a forward model (see Sect. 3.1 for details) that simulates the time evolution of the ice  
20 column to time varying surface conditions. Due to highly diffusive nature of the problem, no high frequency information is retained, and therefore it is not possible to reconstruct a unique solution.

Two inversion methods (see Sects. 3.2.1 and 3.2.2 for details) were used to select  
25 ground surface temperature histories that minimise the RMS error in the simulated temperature profile. The Least Squares QR (LSQR) method produces a single solution that is in some sense a minimum variance solution (actually the sum of minimum

---

## Mill Island warming

J. L. Roberts et al.

---

Title Page

Abstract

Introduction

Conclusions

References

Tables

Figures



Back

Close

Full Screen / Esc

Printer-friendly Version

Interactive Discussion



variance additions to an initial solution) and a more scholastic Particle Swarm Optimisation (PSO) method that produces a distribution of possible solutions. The ground surface temperature history reconstruction using each of these methods is shown in Fig. 4.

As shown in Fig. 4, the measured temperature distribution is consistent with a change in surface energy balance at the site, and there is around a 0.75 K temperature increase between 119 and 19 m (see Table 1). Key details of this site, such as the vertical velocity profile are not known, but reasonable estimates of these values yields a timing of this surface energy budget change of circa 1980/1981 AD  $\pm$  5 yr, and this result is robust to changes in the vertical velocity distribution to values which are probably at the bounds of what is likely. Specifically, there is little difference in the time required for ice to move from the surface to around 60 m depth for either of the velocity profiles considered, the resulting age profiles down the borehole only start differing significantly at greater depths (see Fig. 5).

In general the inverse surface ground temperature reconstructions from the two methods (LSQR and PSO) agree well (see Fig. 4), although the LSQR method tends to have smoothed out the transition around 1980 AD and over estimated the very recent (last 5 yr) temperature increase. This is, at least in part, due to the least variance (in a 2-norm sense) nature of a LSQR solution for under-determined problems (Golub and Loan, 1990).

The PSO solution (Fig. 4) shows a fairly constant median surface ground temperature history up until circa 1980 AD and then shows an approximately linear increase post 1980 AD at a rate of 0.37 Kdecade<sup>-1</sup>. This rate is large by Antarctic standards and is only exceeded in regions of the Antarctic Peninsula (Turner et al., 2005). The PSO method used piecewise linear reconstructions of the surface temperature history (with 4 linear segments) and was free to evolve to include large magnitude but short duration variations. Such variations would be fairly quickly diffused away. The spread of the PSO surface temperature reconstruction (as shown by the percentile bands in Fig. 4) are a reflection of both this potential for short term variability, the additional time

**Mill Island warming**

J. L. Roberts et al.

[Title Page](#)[Abstract](#)[Introduction](#)[Conclusions](#)[References](#)[Tables](#)[Figures](#)[◀](#)[▶](#)[◀](#)[▶](#)[Back](#)[Close](#)[Full Screen / Esc](#)[Printer-friendly Version](#)[Interactive Discussion](#)

for thermal diffusion to act deeper into the borehole, and the relative lack of constraining observations deeper into the borehole. This last point is due to a combination of both the physical spacing of the temperature observations and the non-linear mapping between depth and age, so that the same physical distance represents longer epochs deeper into the borehole.

## 5 Discussion

There is insufficient evidence to attribute the changed surface energy budget at the borehole site to any individual mechanism. Indeed several processes are likely to have contributed. In particular, possible mechanisms contributing to the recently increased surface energy budget include an increase in air temperature due to local or regional scale processes, a change in the radiative balance and latent heat processes.

Roberts et al. (2001) demonstrated regional scale coherence between coastal Antarctic sites that span Mill Island, in particular between multi-decadal averaged Law Dome summer temperatures and a similarly averaged moisture balance for Ace Lake in the Vestfold Hills. Furthermore, van Ommen and Morgan (2010) shows a similar spatial scale climate teleconnection, in this case between Law Dome annual accumulation and south west Western Australia rainfall. In addition, the multi-decadal high accumulation at Law Dome starting circa 1970 AD is unique in the last 750 yr (van Ommen and Morgan, 2010). Together, this shows that suitable regional scale spatial climate coherence exists over this region, and that current climate conditions are unusual over the last several hundred years. Therefore, while local processes (see below) might be directly responsible for the changed surface energy budget, ultimately regional scale changes are likely to be contributing to these changed local processes.

More local scale processes that will directly influence the air temperature are changes in air/sea exchanges, which are strongly moderated by the presence of either sea-ice or a more substantial ice shelf. Mill Island is on the periphery of the Shackleton Ice Shelf, so any changes in its extent has the potential to significantly alter the local

## Mill Island warming

J. L. Roberts et al.

Title Page

Abstract

Introduction

Conclusions

References

Tables

Figures



Back

Close

Full Screen / Esc

Printer-friendly Version

Interactive Discussion



atmospheric conditions. Specifically, there has been an approximate 17% decrease in the area of the Shackleton Ice Shelf between 1956 and 2006, with most of the changes occurring in the region bounded by Mill Island and Bowman Island (Young and Gibson, 2012), where the ice shelf has retreated to the Antarctic coast between these two islands.

Changes to the amount of cloud cover at the site, or the timing of cloud coverage on both diurnal and annual time scales has the potential to contribute to the heat budget. In particular, an increase in either night time cloud cover or atmospheric water content, would decrease the radiative losses at this site and would contribute to annual average warming. Due to the limited period of availability of satellite data, which does not extend to before the observed change in the surface energy budget, this factor can not be directly assessed, although analysis of atmospheric reanalysis products would offer some insight.

Observations made by the field party drilling the ice core over the 2009/2010 austral summer indicate that summer daytime heating of the open ocean surface produced evaporation and a sea-breeze that resulted in a marine fog layer at near surface level over the summit that persisted during the afternoon into the evening. A rime coating covered the surface, hence raising the liquid water deposition at the site. However, the marine fog reduced daytime incident radiation and surface melting and early evening radiative loss. In contrast, on days when the sea-breeze did not occur a combined geostrophic wind from the southerly quadrant prevailed and kept the surface cloud free. Under these conditions, surface melting occurs in summer.

Finally, latent heat processes related to the freezing of liquid water deposited at the site has the potential to significantly alter the energy budget. In particular due to the relative magnitudes of the latent heat of freezing and the specific heat content of firn, freezing of liquid water has the capacity to raise 160 times its own mass of firn by 1 K (Patterson, 1994). Therefore the observed 0.75 K temperature rise over the bottom 100 m of the borehole could be accounted for by an additional  $6 \text{ kg m}^{-2} \text{ yr}^{-1}$  of liquid water deposition at the site. Potential sources for the liquid deposition include,

**Mill Island warming**

J. L. Roberts et al.

[Title Page](#)[Abstract](#)[Introduction](#)[Conclusions](#)[References](#)[Tables](#)[Figures](#)[◀](#)[▶](#)[◀](#)[▶](#)[Back](#)[Close](#)[Full Screen / Esc](#)[Printer-friendly Version](#)[Interactive Discussion](#)

but are not limited to, liquid deposition associated with the marine fog (indicated by corresponding rime coatings) or alternatively from wind blown sea-spray. Salinity levels at the site are relatively high compared to other Antarctic sites, with mean salinity levels around 5 ppm. Therefore small changes in the mode of delivery of this salt to the site (i.e. direct sea spray compared with salt dissolved in snowfall) have the potential to contribute significantly to the altered surface energy budget.

## 6 Conclusions

The temperature profile down an ice borehole into the Mill Island icecap shows a distinct change of gradient between 49 and 69 m below the surface. Numerical modelling suggests that this temperature profile is due to a change in the surface energy budget that occurred around 1980/1981 AD  $\pm$  5 yr. This increase in the surface energy budget since circa 1980 has resulted in a warming of around  $0.37 \text{ Kdecade}^{-1}$ , although care must be taken in interpreting this effective ground surface temperature reconstruction. Factors that may have contributed to this trend of increasing ground surface temperature include an increase in air temperature from either local or regional influences, a change in the surface radiation budget and an increase in the amount (in either absolute or relative terms) of liquid water deposition. A synthesis of climate reconstructions, beyond the scope of the present work, may help to clarify the relative importance of these factors at the Mill Island site.

### Mill Island warming

J. L. Roberts et al.

Title Page

Abstract

Introduction

Conclusions

References

Tables

Figures

◀

▶

◀

▶

Back

Close

Full Screen / Esc

Printer-friendly Version

Interactive Discussion



## Nomenclature

- $C$  Specific heat capacity ( $\text{J kg}^{-1} \text{K}^{-1}$ )  
 $f$  Firn densification energy term ( $\text{J m}^{-3} \text{s}^{-1}$ )  
 $T$  Temperature (K)  
 $t$  Time (s)  
 $w$  vertical velocity ( $\text{m s}^{-1}$ )  
 $z$  vertical distance (m)

## Greek Characters

- $\kappa$  Thermal conductivity ( $\text{W m}^{-1} \text{K}^{-1}$ )  
 $\rho$  Firn/ice density ( $\text{kg m}^{-3}$ )

*Acknowledgements.* The Australian Antarctic Division provided funding and logistical support (ASAC 1236). This work was supported by the Australian Government's Cooperative Research Centres Programme through the Antarctic Climate and Ecosystems Cooperative Research Centre (ACE CRC).

## References

- Golub, G. and Loan, C. V.: Matrix Computations, 2nd edn., The Johns Hopkins University Press, Baltimore, 1990. 2583
- 10 Jouzel, J., Masson-Delmotte, V., Cattani, O., Dreyfus, G., Falourd, S., Hoffmann, G., Minster, B., Nouet, J., Barnola, J. M., Chappellaz, J., Fischer, H., Gallet, J. C., Johnsen, S., Leuenberger, M., Loulergue, L., Luethi, D., Oerter, H., Parrenin, F., Raisbeck, G., Raynaud, D., Schilt, A., Schwander, J., Selmo, E., Souchez, R., Spahni, R., Stauffer, B., Stefansen, J. P., Stenni, B., Stocker, T. F., Tison, J. L., Werner, M., and Wolff, E. W.: Orbital and millennial Antarctic climate variability over the past 800 000 years, *Science*, 317, 793–796, doi:10.1126/science.1141038, 2007. 2576
- 15 Mann, M. and Jones, P.: Global surface temperatures over the past two millennia, *Geophys. Res. Lett.*, 30, 1820, doi:10.1029/2003GL017814, 2003. 2576, 2577

## Mill Island warming

J. L. Roberts et al.

Title Page

Abstract

Introduction

Conclusions

References

Tables

Figures

◀

▶

◀

▶

Back

Close

Full Screen / Esc

Printer-friendly Version

Interactive Discussion



**Mill Island warming**

J. L. Roberts et al.

Title Page

Abstract

Introduction

Conclusions

References

Tables

Figures

I◀

▶I

◀

▶

Back

Close

Full Screen / Esc

Printer-friendly Version

Interactive Discussion



- Mann, M., Zhang, Z., Hughes, M., Bradley, R., Miller, S., Rutherford, S., and Ni, F.: Proxy-based reconstructions of hemispheric and global surface temperature variations over the past two millennia, *Proc. Natl. Acad. Sci. USA*, 105, 13252–13257, 2008. 2576, 2577
- 5 Martins, J., Sturdza, P., and Alonso, J.: The Complex-step derivative approximation, *ACM T. Math. Software*, 29, 245–262, 2003. 2580
- Neukom, R. and Gergis, J.: Southern Hemisphere high-resolution palaeoclimate records of the last 2000 years, *The Holocene*, 22, 501–524, 2012. 2576
- Paige, C. and Saunders, M.: LSQR: an algorithm for sparse linear equations and sparse least squares, *ACM T. Math. Software*, 8, 43–71, 1982. 2580
- 10 Patterson, W.: *The Physics of Glaciers*, 3rd Edn., Butterworth Heinemann, Oxford, 1994. 2578, 2579, 2585
- Pedersen, M. and Chipperfield, A.: Simplifying particle swarm optimization, *Appl. Soft Comput.*, 10, 618–628, doi:10.1016/j.asoc.2009.08.029, 2010. 2581
- Roberts, D., van Ommen, T. D., McMinn, A., Morgan, V., and Roberts, J. L.: Late-Holocene East Antarctic climate trends from ice-core and lake-sediment proxies, *The Holocene*, 11, 117–120, 2001. 2577, 2584
- 15 Scambos, T., Bohlander, J., and Raup, B.: Images of Antarctic ice shelves, Tech. rep., National Snow and Ice Data Center, available at: [http://nsidc.org/data/iceshelves\\_images/](http://nsidc.org/data/iceshelves_images/) (last access: 17 July 2012), 2011. 2591
- 20 Turner, J., Colwell, S., Marshall, G., Lachlan-Cope, T., Carleton, A., Jones, P., Reid, V. L. P., and Iagovkina, S.: Antarctic climate change during the last 50 years, *Int. J. Climatol.*, 25, 279–294, 2005. 2583
- van Ommen, T. and Morgan, V.: Snowfall increase in coastal East Antarctica linked with South-west Western Australian drought, *Nat. Geosci.*, 3, 267–272, 2010. 2584
- 25 van Ommen, T., Morgan, V., Jacka, T., Woon, S., and Elcheikh, A.: Near-surface temperatures in the Dome Summit South (Law Dome, East Antarctica) borehole, *Ann. Glaciol.*, 29, 141–144, 1999. 2579
- Young, N. and Gibson, J.: A century of change in the Shackleton and West ice shelves, East Antarctica, *Global Planet. Change*, submitted, 2012. 2585

## Mill Island warming

J. L. Roberts et al.

Title Page

Abstract

Introduction

Conclusions

References

Tables

Figures

I◀

▶I

◀

▶

Back

Close

Full Screen / Esc

Printer-friendly Version

Interactive Discussion

**Table 1.** Observed borehole temperature distribution.

Depth below 2011 surface (m)	Temperature (°C)
0	−3.2750
9.05	−14.2750
14.06	−13.8625
19.07	−13.8625
21.07	−13.9250
23.07	−13.9625
25.07	−14.0000
27.07	−14.0500
29.07	−14.0750
31.09	−14.1125
33.09	−14.1500
35.11	−14.1750
37.11	−14.2000
39.11	−14.2250
44.125	−14.3000
49.14	−14.3500
69.17	−14.4875
89.24	−14.5500
109.30	−14.6000
119.31	−14.6125

## Mill Island warming

J. L. Roberts et al.

Title Page

Abstract

Introduction

Conclusions

References

Tables

Figures

I◀

▶I

◀

▶

Back

Close

Full Screen / Esc

Printer-friendly Version

Interactive Discussion

**Table 2.** Sensitivity of PSO median solution to the RMS threshold.

RMS threshold	RMS error in median	Maximum error in median
0.2	$2.92 \times 10^{-2}$	$7.17 \times 10^{-2}$
0.1	$1.71 \times 10^{-2}$	$4.38 \times 10^{-2}$
0.05	$1.49 \times 10^{-2}$	$2.30 \times 10^{-2}$
0.025*	$1.40 \times 10^{-2}$	$2.83 \times 10^{-2}$
0.0125*	$1.27 \times 10^{-2}$	$2.87 \times 10^{-2}$

\* Denotes a skewed distribution.

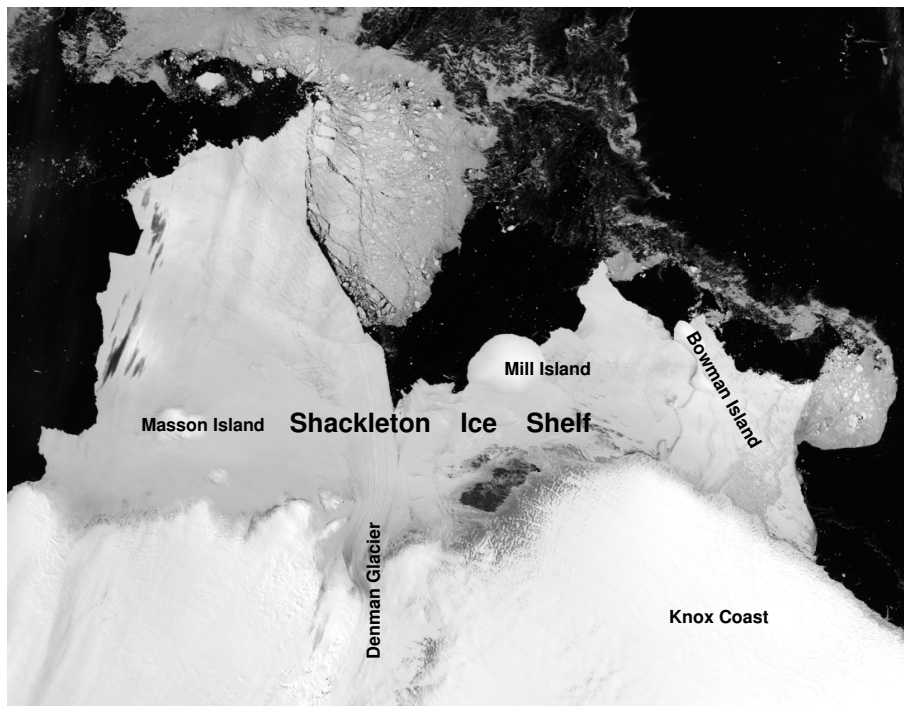


**Fig. 1.** Moderate Resolution Imaging Spectroradiometer (MODIS) image of Mill Island and surrounds, from Scambos et al. (2011) with modification.

**Mill Island warming**

J. L. Roberts et al.

Title Page

Abstract Introduction

Conclusions References

Tables Figures

◀ ▶

◀ ▶

Back Close

Full Screen / Esc

Printer-friendly Version

Interactive Discussion



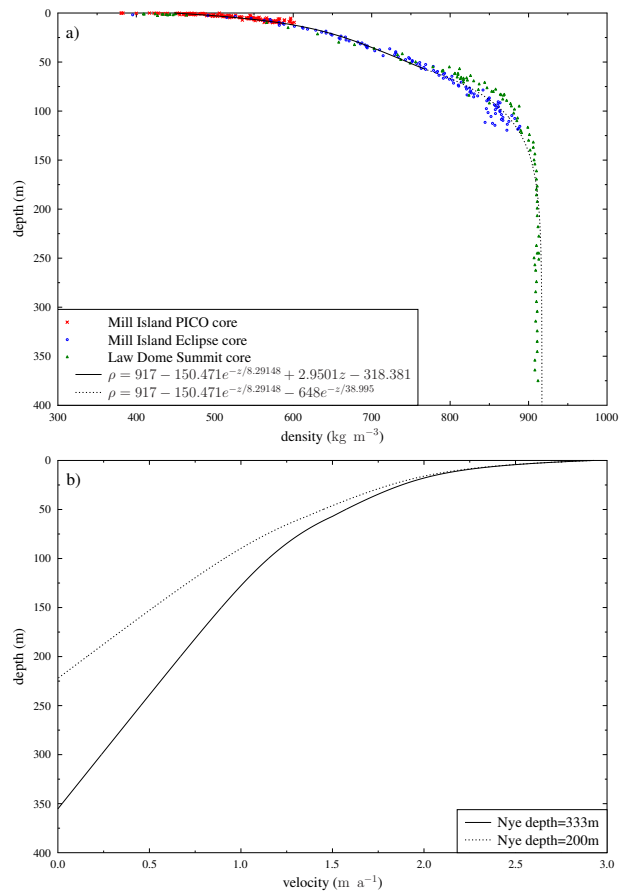


**Fig. 2. (a)** Density and **(b)** velocity profiles used in the ground surface temperature reconstruction.

Title Page

Abstract

Introduction

Conclusions

References

Tables

Figures

◀

▶

◀

▶

Back

Close

Full Screen / Esc

Printer-friendly Version

Interactive Discussion



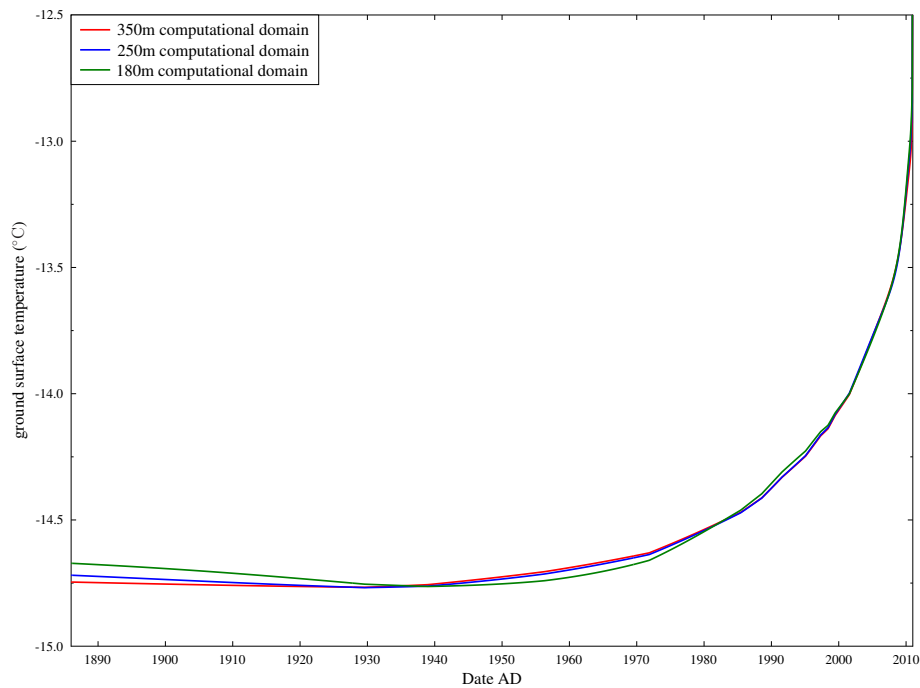


**Fig. 3.** Sensitivity of the reconstructed ground surface temperature reconstruction to the depth of the computation domain, and hence the position of the zero heat flux boundary.

**Mill Island warming**

J. L. Roberts et al.

Title Page

Abstract Introduction

Conclusions References

Tables Figures

◀ ▶

◀ ▶

Back Close

Full Screen / Esc

Printer-friendly Version

Interactive Discussion



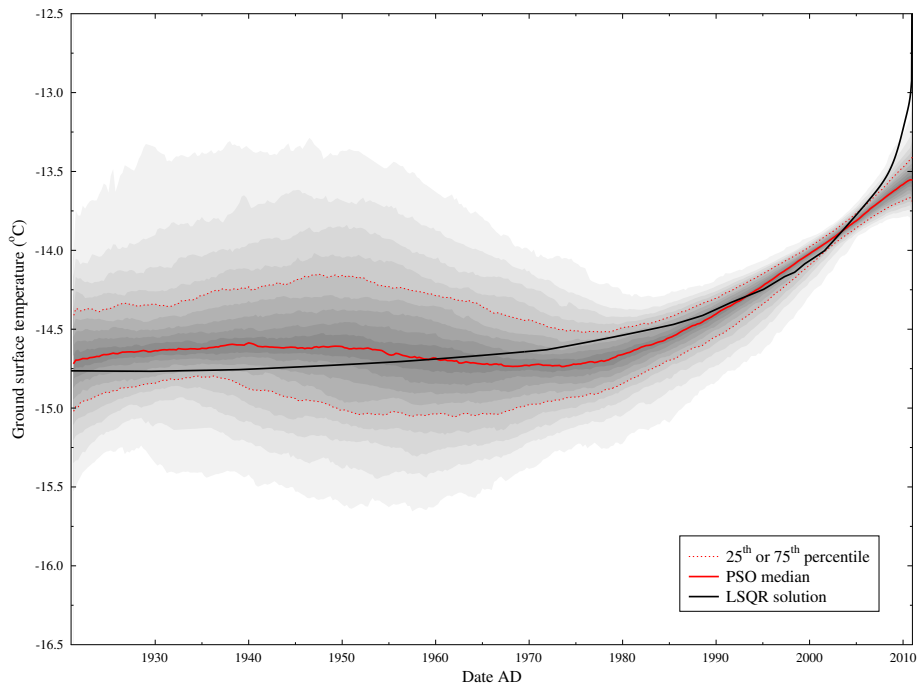


**Fig. 4.** Reconstructed ground surface temperature history using PSO optimisation with a RMS threshold of  $0.05^{\circ}\text{C}$  (red) and LSQR solution (black). The shading increments in 5% percentiles of the PSO distribution.

**Mill Island warming**

J. L. Roberts et al.

Title Page

Abstract Introduction

Conclusions References

Tables Figures

◀ ▶

◀ ▶

Back Close

Full Screen / Esc

Printer-friendly Version

Interactive Discussion



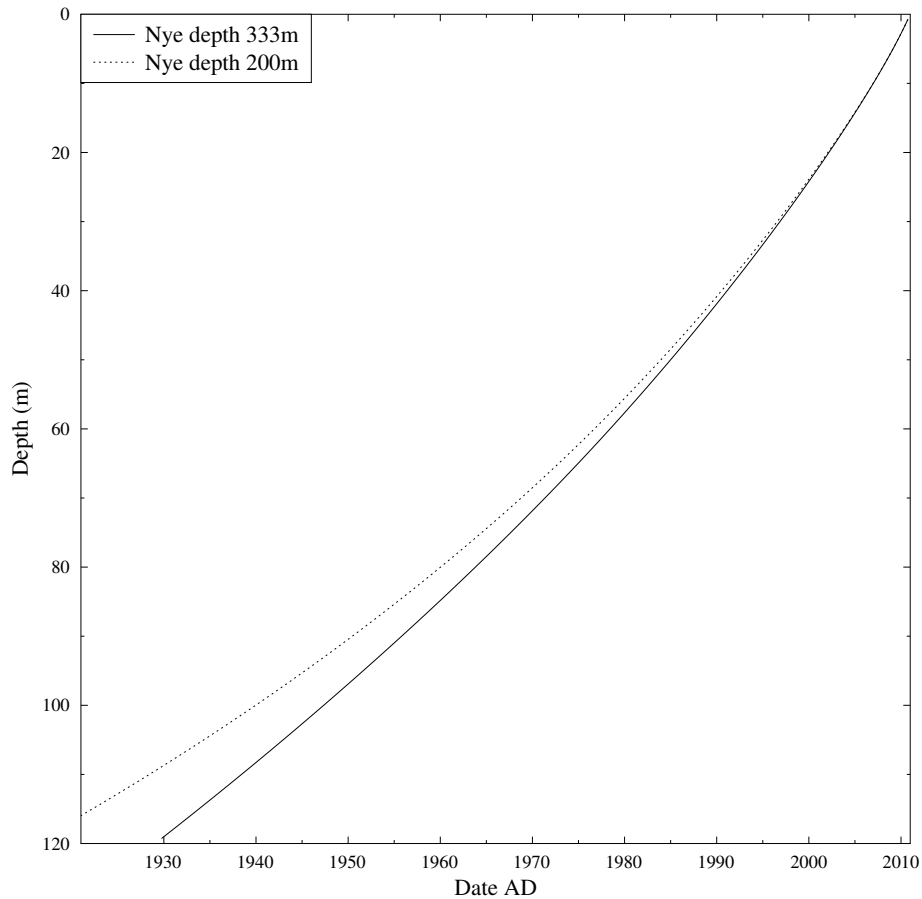


**Fig. 5.** The influence of assumed vertical velocity profiles on the age distribution down the Mill Island borehole.

**Mill Island warming**

J. L. Roberts et al.

Title Page

Abstract Introduction

Conclusions References

Tables Figures

◀ ▶

◀ ▶

Back Close

Full Screen / Esc

Printer-friendly Version

Interactive Discussion

